

Unified Video Editing as Temporal Reasoner

Anonymous CVPR submission

Paper ID 957



Figure 1. VideoCoF’s video editing capabilities emerge from its **seeing, reasoning, then editing framework**. Trained on only **50k** data (33 frames), this teaser shows multi-instance editing and robust $4\times$ length generalization.

Abstract

Existing video editing methods face a critical trade-off: expert models offer precision but rely on task-specific priors like masks, hindering unification; conversely, unified

temporal in-context learning models are mask-free but lack explicit spatial cues, leading to weak instruction-to-region mapping and imprecise localization. To resolve this conflict, we propose **VideoCoF**, a novel **Chain-of-Frames** approach inspired by Chain-of-Thought reasoning. VideoCoF

004
005
006
007
008

enforces a “see → reason → edit” procedure by compelling the video diffusion model to first predict **reasoning tokens** (edit-region latents) before generating the target video tokens. This explicit reasoning step removes the need for user-provided masks while achieving precise instruction-to-region alignment and fine-grained video editing. Furthermore, we introduce a RoPE alignment strategy that leverages these reasoning tokens to ensure motion alignment and enable length extrapolation beyond the training duration. We demonstrate that with a minimal data cost of only 50k video pairs, VideoCoF achieves state-of-the-art performance on VideoCoF-Bench, validating the efficiency and effectiveness of our approach.

1. Introduction

The development of Video Diffusion Models (VDM) [12, 27, 33, 37] has enabled high-fidelity video generation across a wide range of concepts. Building on these advances, video editing methods support users in designing video by adding [26], removing [15, 43], swapping [6, 36] visual concepts, and performing global style transformation [39].

Current video editing methods mainly follow two strategies: (i) **expert models** [1, 15, 26, 36, 41], which use adapter-based modules to feed *external masks* into the video generation model, yielding precise, localized edits but requiring additional inputs and per-task overhead; and (ii) **unified temporal in-context learning models** [9, 16, 38], which concatenate source tokens with noised edit tokens along the temporal dimension and use self-attention mechanism to guide the edit. However, without explicit spatial cues, these models often exhibit weak accuracy, especially in cases that need multi-instance recognition or spatial reasoning (Fig. 2, left). In short, there is a *trade-off*: expert models are accurate but mask-dependent, while unified in-context models are mask-free but less precise; This raises a critical question: **Can we maintain former’s precision and latter’s unification without the mask dependency?**

Inspired by Chain-of-Thought (CoT) multi-step reasoning [30], we *compel* the video diffusion model to first predict the edit region and then perform the edit, enforcing a “**see → reason → edit**” procedure. Accordingly, we propose **VideoCoF**, a Chain-of-Frames approach that predicts **reasoning tokens** (edit-region latents) before generating the target video tokens, thereby removing the need for user-provided masks while achieving precise instruction-to-region alignment. To explicitly model the reasoning process, we leverage visual grounding, which is naturally suited to simulating reasoning about the edit region. Empirically, we find a soft, gradually highlighted grayscale region is the most effective reasoning format. Additionally, we introduce a RoPE alignment strategy. By explicitly accounting for the reasoning latent, we reset the temporal indices

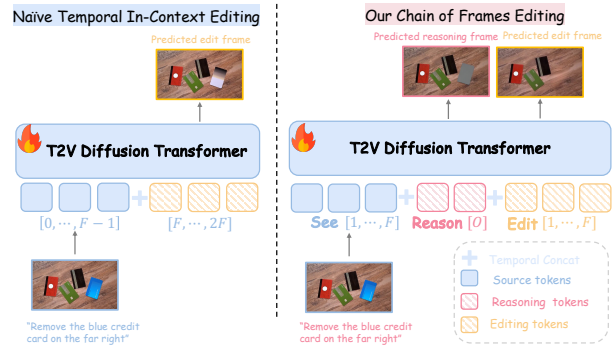


Figure 2. Illustration of the difference between previous methods and our VideoCoF. We enhances the editing accuracy by forcing the video diffusion model to first predict the editing area, and then perform the editing.

of the edited video’s rotary position embeddings to match those of the source segment, ensuring motion alignment and length extrapolation.

To holistically evaluate fine-grained video editing, we further construct VideoCoF-Bench. VideoCoF trained on only **50k** video pairs, outperforms a strong baseline ICVE [16] that uses $\sim 1M$ pretraining videos plus 150k for SFT. Specifically, we improves the instruction-following score by **+15.14%** and the success ratio by **+18.8%**. Our contributions can be summarized as follows:

- We propose VideoCoF, the first framework to introduce a Chain of Frames approach to video editing, enabling temporal reasoning for fine-grained video editing.
- Building on VideoCoF, we explore an effective reasoning format for video diffusion models, and introduce a RoPE alignment strategy that allowing generalization to longer frames exceeding the training duration.
- We demonstrate that with a minimal data cost (only **50k** video pairs), we achieve state-of-the-art quantitative and qualitative performance on VideoCoF-Bench, validating the efficiency and effectiveness of our approach.

2. Related Work

Video Editing Methods. Early training-free video editing methods [21, 33] used inversion and consistency techniques (e.g., attention manipulation [21] or optical flow [5]) but often lack precise control and struggle with complex edits. Data-driven, training-based methods [2, 4] have become the focus, offering higher quality and edit diversity. A concurrent line of research [18, 29, 40] integrates MLLMs to guide the editing process, though this adds significant training and inference cost, which our pure VDM approach avoids.

In-Context Video Editing. Recently, in-context learning (ICL) has emerged as a promising paradigm for unified editing [10, 35, 42]. Methods like UNIC [38] and ICVE [16] concatenate video conditions along the temporal axis

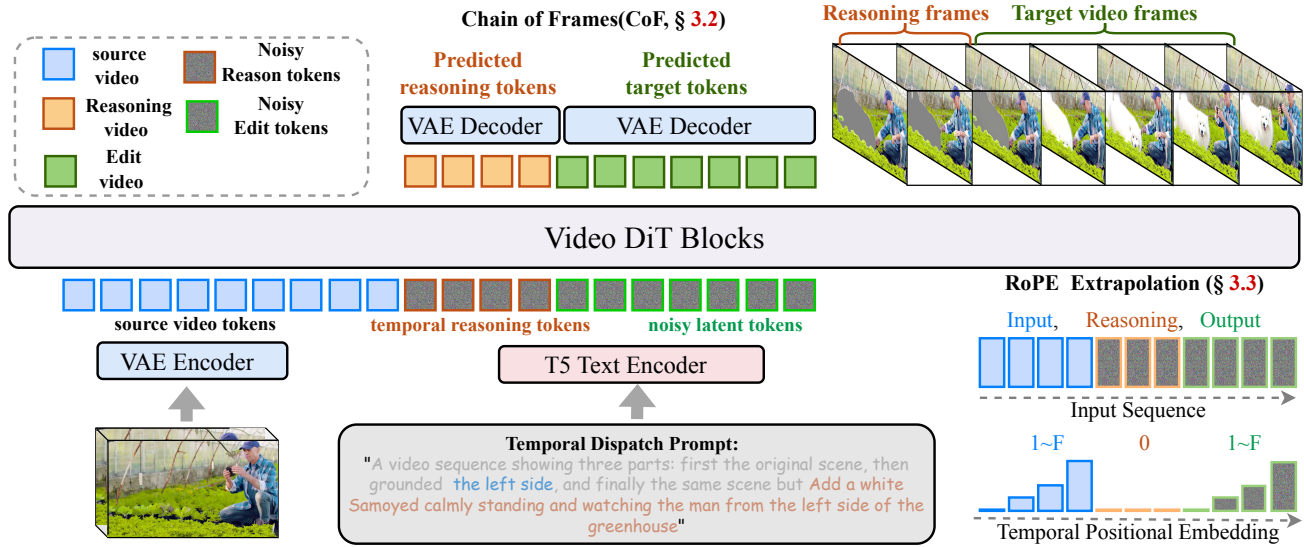


Figure 3. Overview of VideoCoF framework. Our model processes source (blue), reasoning (orange), and target (green) tokens in a unified sequence to “reason” then “edit”. **Bottom right:** Our RoPE design enables length extrapolation.

to perform ICL. However, these methods are often limited by mask requirements [38] or, as we identify, suffer from fundamental issues with editing accuracy and a lack of length extrapolation due to their naive temporal concatenation. While EditVerse [9] also explored unified in-context learning, it was built on a LLaMA-style DiT backbone, whereas our work explores these capabilities within a standard video diffusion transformer.

Chain of Thought in Vision. Chain-of-Thought (CoT) prompting [11, 30] elicits multi-step reasoning in LLMs by having them “think step-by-step.” This concept of emergent reasoning has also been identified in large video generative models [3, 31] that can solve visual puzzles. However, how to leverage visual reasoning for the task of unified video editing remains unexplored. In this work, we investigate whether generative video models can perform a “chain of frames” reasoning to achieve this.

3. Methods

3.1. VideoCoF Framework

As illustrated in Figure 3, VideoCoF employs a VideoDiT [27] for unified video editing. We model editing as a reasoning-then-generation process: the model first reasons where to edit, then generates the intended content in that area. We call this process “**Chain of Frames (CoF)**” (Sec 3.2). All visual inputs (source, reasoning, and target frames) are encoded separately by a Video VAE and then concatenated temporally. The unified frame sequence is then fed into the model, performing unified in-context learning via self-attention and language control via cross-attention. To enable video alignment and variable-length inference, we revisit the design of positional encoding. We adapt the tem-

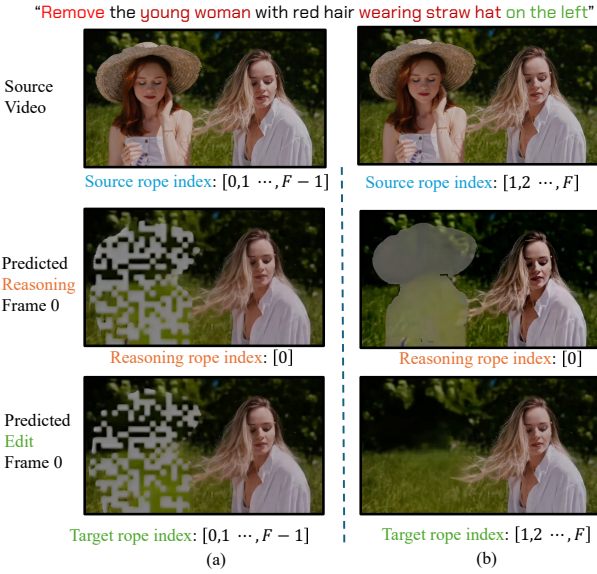
poral RoPE for source-to-target alignment and reasoning tokens’ RoPE for explicit spatial guidance (Sec 3.3). Subsequent sections detail the insights behind our design choices and data curation pipeline (Sec 3.5).

3.2. Chain of Frames

Seeing, Reasoning, then Editing. Previous video in-context editing methods, such as UNIC [38], ICVE [16], or EditVerse [9], perform in-context learning by temporally concatenating clean source video tokens with noised editing video tokens. However, this approach lacks an explicit constraint mapping the editing instruction to the specific editing region, leading to editing accuracy problems, as shown in Fig 2. Recently, VDM have been shown to possess reasoning capabilities, as demonstrated in [31]. Inspired by this, we explicitly model the reasoning tokens, forcing the model to actively learn the relationship between the editing instruction and the target edit region first. The edit is then executed *after* reasoning, following a “see, reason, then edit” process.

Inspired by Chain of Thought prompting in Large Language Models (LLMs) [30], we argue that a video generative model should also have an analogous chain-reasoning ability. Given the generative priors in video editing, the visual-chain should be progressive, moving from the original video to a visual reference of the editing region, and finally to the edited video. Visual grounding is naturally suitable for this representation. Since video diffusion models are often insensitive to grounding masks (black or white pixels). Therefore, we choose to use a gray highlight to delineate the “grounding region,” which is also evidence in [7]. Finally, the gray-highlighted area as the ground truth for the reasoning frames, teaching the diffusion model to

126
127
128
129
130
131
132
133
134
135
136
137
138
139
140
141
142
143
144
145
146
147
148
149
150
151
152
153
154
155
156
157

**Figure 4.** How our RoPE design avoid index collision.

reason about where the edit should occur.

Consequently, the entire video editing task is reformulated as a chained process: first “seeing” the original video, then “reasoning” by predicting the grounding region, and finally “editing” to generate the new video content within that specified area. We call this **Chain of Frames (CoF)**.

Let $\mathcal{E}(\cdot)$ denote the video VAE encoder. We use F and L for frames in the source/target and reasoning latent space, respectively, and denote channel, height, and width by C , H , and W . Given a triplet source-reasoning-target video pair $\{\mathbf{s}, \mathbf{r}, \mathbf{e}\}$, we first encode them into latent representations. The source \mathbf{s} and target video \mathbf{e} yield latent $z_s = \mathcal{E}(\mathbf{s})$ and $z_e = \mathcal{E}(\mathbf{e})$, both with shape $\mathbb{R}^{F \times C \times H \times W}$. The reasoning video \mathbf{r} yields a latent $z_r = \mathcal{E}(\mathbf{r})$ with shape $\mathbb{R}^{L \times C \times H \times W}$. This separate encoding ensures intra-causal relations and inter-video independence. Then, we perform temporal concatenation to get the unified representation:

$$\mathbf{z}_{full}^{(t)} = \underbrace{z_s^{(0)}}_{\text{seeing}} \parallel \underbrace{z_r^{(t)}}_{\text{reasoning}} \parallel \underbrace{z_e^{(t)}}_{\text{editing}} \in \mathbb{R}^{(F+L+F) \times C \times H \times W}, \quad (1)$$

where the $z_s = \mathbf{z}_{0:F-1}^{(0)}$ denotes anchoring the source video latent at timestep 0. $z_r = \mathbf{z}_{F:F+L-1}^{(t)}$ and $z_e = \mathbf{z}_{F+L:2F+L-1}^{(t)}$ mean the reasoning and target noised video latents at timestep t. At each denoising step, only the $L + F$ reasoning and target frames are denoised, and the source video latents are kept clean.

3.3. RoPE Design for Length Extrapolation

In VideoDiT, 3D factorized RoPE [23] provides spatio-temporal positions. A naive in-context learning approach applies sequential temporal indices (e.g., 0 to $2F - 1$) across

concatenated source and target videos. However, this hinders video length extrapolation, as the model overfits to a static $[0, F - 1] \rightarrow [F, 2F - 1]$ mapping and fails to generalize to videos longer than F frames.

A better strategy is to repeat the temporal indices. For our CoF triplet (consider $L = 1$ for reasoning frame), a straightforward reset configuration is to assign temporal indices: $[0, F - 1]$ to the source, “0” to the reasoning frame, and $[0, F - 1]$ to the target.

However, as illustrated in Figure 4 (a), this naive reset leads to index collisions at temporal position 0, shared by the source, reasoning, and target frames. This overlap introduces visual artifacts that propagate from the reasoning tokens into the first target frame.

To resolve this index collision, we set the temporal indices for both the source video and the target video to the range $[1, F]$, while keeping the reasoning frame’s temporal index at 0. This isolates the reasoning token and prevents artifact leakage while maintaining length generalization.

3.4. Training and Inference Paradigm

Algorithm 1 Chain of Frame (CoF) Training

Input: Dataset \mathcal{D} with tuples $(\mathbf{z}_s^{(0)}, \mathbf{z}_r^{(0)}, \mathbf{z}_e^{(0)}, \mathbf{c})$

Output: Fine-tuned parameters θ

```

foreach minibatch  $(\mathbf{z}_s^{(0)}, \mathbf{z}_r^{(0)}, \mathbf{z}_e^{(0)}, \mathbf{c}) \sim \mathcal{D}$  do
    foreach sample in minibatch do
         $\mathbf{z}_{full}^{(0)} \leftarrow \mathbf{z}_s^{(0)} \parallel \mathbf{z}_r^{(0)} \parallel \mathbf{z}_e^{(0)}$  Sample  $t \sim \mathcal{U}[0, 1]$ 
        Sample  $\varepsilon \sim \mathcal{N}(\mathbf{0}, \mathbf{I})$  with the same shape  $\mathbf{z}_{full}^{(0)}$   $\mathbf{v} \leftarrow (\varepsilon - \mathbf{z}_{full}^{(0)})$ 
         $\mathbf{z}_{r,e}^{(t)} \leftarrow (1 - t)(\mathbf{z}_r^{(0)} \parallel \mathbf{z}_e^{(0)}) + t(\varepsilon_{F:2F+L-1})$   $\mathbf{z}^{(t)} \leftarrow \mathbf{z}_s^{(0)} \parallel \mathbf{z}_{r,e}^{(t)}$ 
         $\hat{\mathbf{v}} \leftarrow \mathbf{F}_\theta(\mathbf{z}^{(t)}, t, \mathbf{c})$ 
         $\mathcal{L} \leftarrow \frac{1}{L+F} \sum_{i=F}^{2F+L-1} \|\mathbf{v}_i - \hat{\mathbf{v}}_i\|_2^2$ 
    Update  $\theta$  using gradients of  $\mathcal{L}$ 

```

Given a concatenated full latent sequence $\mathbf{z}_{full}^{(0)} = \text{TemporalConcat}(\mathbf{z}_s^{(0)}, \mathbf{z}_r^{(0)}, \mathbf{z}_e^{(0)})$, we treat the reasoning+editing block as the generation target during training.

Given timestep $t \in [0, 1]$ and Gaussian noise $\varepsilon \sim \mathcal{N}(\mathbf{0}, \mathbf{I})$, we only progressively noise the reasoning and editing parts, $\mathbf{z}_{r,e}^{(t)} = (1 - t)(\mathbf{z}_r^{(0)} \parallel \mathbf{z}_e^{(0)}) + t\varepsilon_{F:2F+L-1}$, and form the model input $\mathbf{z}^{(t)} = \mathbf{z}_s^{(0)} \parallel \mathbf{z}_{r,e}^{(t)}$. The target velocity field is $\mathbf{v} = \varepsilon - \mathbf{z}_{full}^{(0)}$. Our model $\mathbf{F}_\theta(\cdot)$ predicts this velocity field from the partially noised input, and we train it by minimizing the mean squared error between predicted and true velocities. Concretely, we only supervise the reasoning and target frames, so the training loss can be written

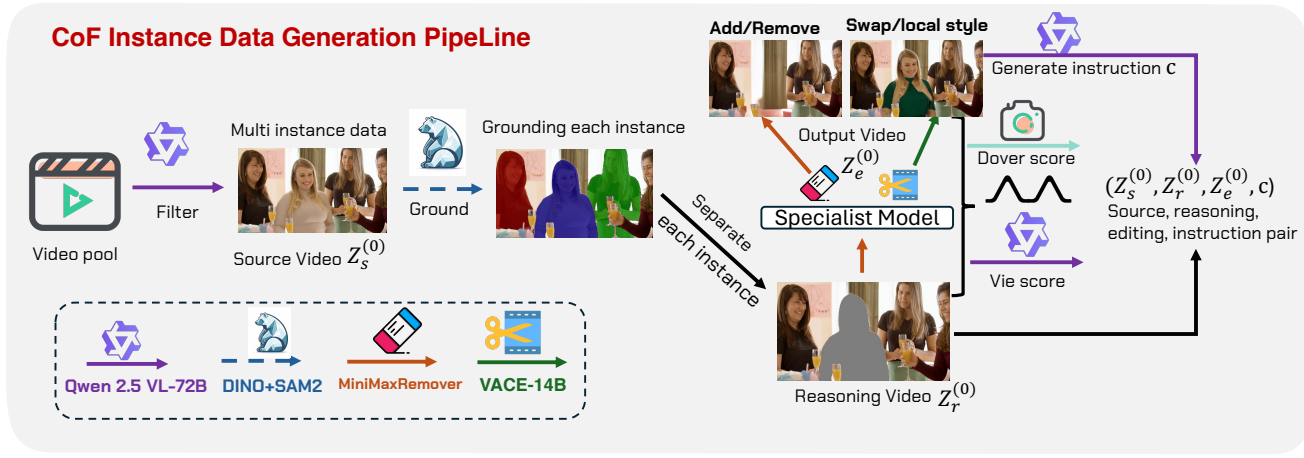


Figure 5. Our data curation pipeline for multi-instance data.

218 in per-frame form as

219
$$\mathcal{L} = \frac{1}{L+F} \sum_{i=F}^{2F+L-1} \left\| \mathbf{v}_i - [\mathbf{F}_\theta(\mathbf{z}^{(t)}, t, \mathbf{c})]_i \right\|_2^2, \quad (2)$$

220 where $[\mathbf{F}_\theta(\mathbf{z}^{(t)}, t, \mathbf{c})]_i$ denotes the model's prediction for
221 frame i and \mathbf{c} is the text condition. The model parameters
222 $\mathbf{F}_\theta(\cdot)$ are updated via a gradient step computed from this
223 loss. The full training procedure is summarized in Algo-
224 rithm 1.225 During inference we initialize the reasoning+editing
226 block from Gaussian noise, $\mathbf{z}_{r,e}^{(1)} \sim \mathcal{N}(\mathbf{0}, \mathbf{I})$ and form the
227 full latent at $t = 1$ by temporal concatenation with the
228 clean source $\mathbf{z}_{full}^{(1)} = \text{TemporalConcat}(\mathbf{z}_s^{(0)}, \mathbf{z}_{r,e}^{(1)})$. An
229 ODE solver guided by our model \mathbf{F}_θ evolves $\mathbf{z}_{full}^{(t)}$ to $\mathbf{z}_{full}^{(0)}$.
230 The source latents $\mathbf{z}_s^{(0)}$ are held fixed during inference, so
231 only the reasoning/editing parts change. We then extract
232 the edited-target latent using the same slicing index as in
233 training: $\mathbf{z}_{edit}^{(0)} = (\mathbf{z}_{full}^{(0)})_{F+L:2F+L-1}$ and decode the final
234 edited video: $\mathbf{x}_{edit} = \mathcal{D}(\mathbf{z}_{edit}^{(0)})$.235

3.5. Video Data Curation

236 The training of our VideoCoF requires a large and di-
237 verse dataset structured as source, reasoning, and edited
238 video triplets. However, existing video editing datasets and
239 methods predominantly focus on single-instance-level ob-
240 ject manipulation. This limitation is a significant barrier, as
241 real-world videos contain complex visual cues, multiple in-
242 teracting instances, and intricate spatial relationships (e.g.,
243 physical left/right, object-to-object interactions). Enabling
244 a generative model to comprehend these complex, instance-
245 level dynamics is a critical step toward true reasoning-based
246 video editing. Therefore, we develop a comprehensive data
247 curation pipeline, illustrated in Figure 5, to specifically gen-
248 erate and process complex, instance-level video data.249 **Instance-Level Curation Pipeline.** Our pipeline begins
250 with a large pool of diverse videos sourced from Pexels251 [20]. First, we employ the Qwen-VL 72B [28] to per-
252 form multi-instance identification, scanning the videos to
253 find scenes that contain multiple, distinct objects. Once
254 these videos are identified, we use Grounding-SAM2 [22]
255 to perform precise segmentation, generating distinct seg-
256 mentation masks for each individual instance. With these
257 instance-specific masks, we generate triplets for a variety of
258 editing tasks:259

- **Object Addition/Removal:** We utilize the Minimaxre-
260 mover [43] to erase a specific instance from the video.
261 The data for object addition is then created by simply re-
262 versing this process.

263

- **Object Swap and Local Style Transfer:** For these tasks,
264 we leverage the VACE 14B [8] in its inpainting mode to
265 fill the specified masked regions. Critically, the creative
266 prompts for these inpainting edits are generated by GPT-
267 4o [19], as we found Qwen-VL 72B's imaginative capa-
268 bilities for this specific task to be limited.

269 **Filtering and Final Dataset.** All generated video pairs are
270 rigorously evaluated to ensure quality. We use the Dover
271 Score [32] to assess aesthetic quality and the VIE Score
272 [13] to measure editing fidelity and coherence. A weighted
273 combination of these scores is used to filter for high-quality,
274 successful edits. Finally, we use this pipeline to filter from
275 the large-scale open-source Señorita 2M [44] dataset, and
276 distill a high-quality subset of 50k videos to supplement our
277 training data. This multi-pronged approach yields our final
278 large-scale dataset, rich in the instance-level complexity re-
279 quired for reasoning-based video editing.280

4. Experiments

281

4.1. Implementation Details.

282 VideoCoF is trained on WAN-14B [27]. We employ a
283 resolution-bucketing strategy to support multiple aspect
284 ratios, using spatial resolutions of 336x592, 400x704,
285 400x752, and 400x944 (and the corresponding vertical
286 variants, e.g., 592x336). Training videos are sourced from

Table 1. We compare VideoCoF with SOTA baselines on VideoCoF-Bench: InsV2V [4], Señorita [44] (an I2V model guided by InsP2P [2]), VACE-14B [8] (using GPT-4o-generated captions), the concurrent ICVE [16] (pretrained on 1M videos and fine-tuned on 150k), and LucyEdit [25]. Despite the extensive training data used by baselines, VideoCoF is fine-tuned on only 50k video pairs and achieves superior instruction-following and success ratio.

Model	GPT-4o Score (avg.)				Perceptual Quality (avg.)		
	Instruct Follow↑	Preservation↑	Quality↑	Success Ratio↑	CLIP-T↑	CLIP-F↑	DINO↑
InsV2V [4]	3.41	6.15	5.51	6.39%	26.19	0.988	0.978
Señorita [44]	3.26	6.30	5.48	10.35%	26.04	0.994	0.988
VACE [8]	7.47	5.82	7.61	26.60%	27.02	0.994	0.990
ICVE [16]	7.79	8.06	8.14	57.76%	27.49	0.992	0.986
Lucy Edit [25]	5.24	6.50	6.37	29.64%	26.98	0.991	0.986
VideoCoF (Ours)	8.97	8.20	<u>7.77</u>	76.36%	28.00	0.992	0.991

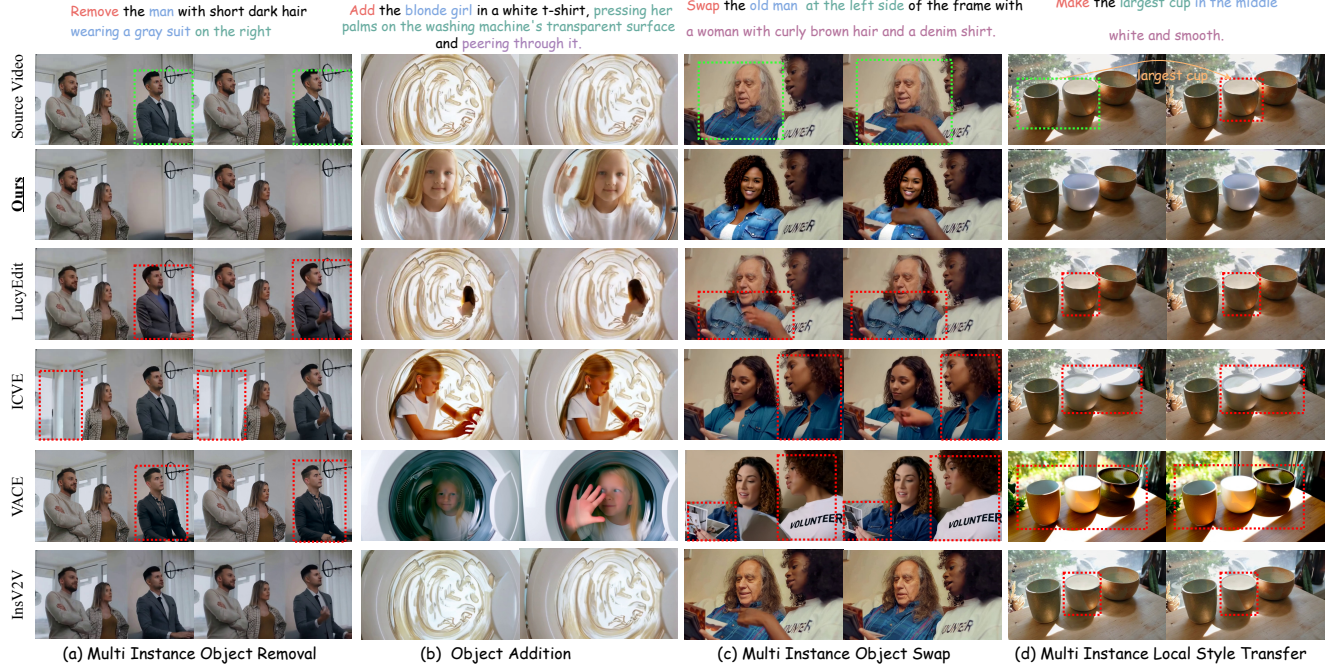


Figure 6. Visual comparsion between our VideoCoF and other methods on diverse video editing tasks.

287 Señorita [44] and are 33 frames long, we only training on
 288 **50k** curated video data finally. Thanks to our RoPE align-
 289 ment design, the model generalizes to longer sequences at
 290 inference (e.g., **141 frames and above**). By default we
 291 use 33 frames source video, 33 frames edited video, and
 292 4 frames reasoning clip. We train with a global batch
 293 size of 16 for approximately 8k iterations, optimizing with
 294 AdamW [17] and a base learning rate of 1×10^{-4} .

295 4.2. VideoCoF-Bench and Experimental Setting

296 **VideoCoF-Bench.** Previous video-editing benchmarks
 297 such as V2VBench [24], TGVE [34], and FIVE-Bench [14]
 298 focus on target-prompt edits and mostly are focused on
 299 class-level object swap. They were mainly designed for
 300 training-free methods and are not suitable for instruction-

301 guided or instance-level video editing. Real-world edit-
 302 ing requires precise instruction understanding, including
 303 instance- and part-level control (e.g., distinguishing mul-
 304 tiple people or left vs. right), and complex reasoning. To
 305 address these gaps, we introduce VideoCoF-Bench. It con-
 306 tains 200 high-quality videos collected from Pexels [20],
 307 covering diverse scenes and both landscape and portrait as-
 308 pect ratios. VideoCoF-Bench includes four task: Object
 309 Removal, Object Addition, Object Swap, and Local Style
 310 Transfer, each with 50 samples. Half of these samples per
 311 task are instance-level cases with instance-focused editing
 312 prompts.

313 **Evaluation Metrics.** To evaluate editing performance on
 314 VideoCoF-Bench, we employ MLLM-as-a-Judge to pro-
 315 vide a holistic evaluation score. This is achieved by prompt-

Table 2. Ablation on Chain of frames and RoPE design.

CoF	Ablation on Chain of frames and RoPE design		
	Naive Temporal in Context		VideoCoF
	X	X	✓
RoPE Design	0–2F–1	0–F–1, 0–F–1	1–F, 0, 1–F
<i>GPT-4o Score</i>			
Instruct Follow↑	8.109	8.064	8.973
Preservation↑	7.930	7.793	8.203
Quality↑	7.394	7.217	7.765
Success Ratio↑*	72.41%	65.52%	76.36%
<i>Perceptual Quality</i>			
CLIP-T↑	26.880	27.088	28.000
CLIP-F↑	0.9907	0.9905	0.9915
DINO↑	0.9857	0.9826	0.9913

316 ing **GPT-4o** [19] to assess multiple criteria given the original video, edited video, and user instruction: (1) Instruction
317 Following (editing accuracy), (2) Preservation (unedited regions), (3) Video Quality. (4) Success ratio: we prompt
318 the GPT-4o to provide a binary Success Ratio (Yes/No) to
319 judge the overall success of the edit. We report three perceptual
320 quality metrics quantify low- and high-level visual similarity
321 between source and target frames: CLIP-T for image–text alignment,
322 CLIP-F for temporal consistency, and
323 DINO for structural consistency.
324

326 4.3. Comparison on VideoCoF-Bench

327 We show qualitative and quantitative comparisons of
328 VideoCoF-Bench in this section. As shown in Table 1,
329 we evaluate VideoCoF against five baseline methods on
330 the VideoCoF-Bench benchmark, which spans four distinct
331 video editing tasks: multi-instance removal, object addition,
332 multi-instance swap, and multi-instance local style transfer.
333

334 Overall, VideoCoF demonstrates the best performance
335 in **Instruct Follow** and **Success Ratio** across all categories.
336 Compared to naive temporal in-context editing approaches
337 like ICVE [16], our method achieves significantly higher
338 success rates and better instruction adherence using only
339 **50k** reasoning pairs, whereas ICVE is pre-trained on 1M
340 samples and fine-tuned on 150k data.

341 Qualitatively (see Figure 6), our method also shows
342 clearer, more faithful edits at the instance level:(a) Multi-
343 instance removal: we precisely remove the right instance
344 while ICVE[16] incorrectly removes the left instance. (b)
345 Object addition: the added girl is correctly placed inside
346 the washing machine, matching the instruction. (c) Object
347 swap: we replace the elderly person’s face and update cloth-
348 ing; Lucy Edit [25] changes only clothing, ICVE fails to dis-
349 ambiguate instances, and VACE often alters non-target peo-
350 ple. (d) Local style (multi-instance): our model correctly
351 identifies and edits the largest cup among several similar ob-
352 jects; other methods either fail to edit or mistakenly edit a
353 bowl. These qualitative examples demonstrate VideoCoF’s
354

**Figure 7.** Length exploration on frames more than training.

stronger instance-level reasoning and higher editing fidelity. 353

354 4.4. Ablation Study

355 To verify our novel Chain of Frames (CoF) design, particu-
356 larly its “reasoning frames” and the RoPE design for length
357 exploration, we conduct an ablation study on the reasoning
358 frames, RoPE alignment strategy and reasoning format. 359

360 **Naive Temporal Incontext VS. CoF.** As shown in Ta-
361 ble 2, we compare VideoCoF against a “Naive Temporal in-
362 context” baseline. This applies temporal in-context learning
363 by using the source video as a condition through temporal
364 concatenation, an approach similar to ICVE [16]. 365

366 In contrast, our approach introduces **reasoning frames**
367 as a core component of the (CoF) design. This ensures the
368 video editing follows a reasoning process, i.e., forcing the
369 model to predict the editing region first and then execute the
370 versatile edit within that specific area. 371

372 The efficacy of this design is evident when comparing
373 the first ($[0, 2F - 1]$) and third (VideoCoF) columns in Ta-
374 ble 2. The inclusion of CoF brings substantial gains: the
375 instruct follow score increases by 10.65% and the success
376 ratio improves by 5.46%. Furthermore, the 4.16% increase
377 in CLIP-T confirms that our reasoning frames effectively
378 enhance the model’s editing accuracy and precision. 379

380 **Rope Design for length Extrapolation.** As illustrated in
381 Fig 7, the naive approach ($[0, 2F - 1]$) only learns a fixed
382 temporal mapping (e.g., mapping frame 0_{th} to frame 33_{th}).
383 This prevents length extrapolation, causing severe degra-
384 dation (blurriness, motion misalignment, and artifacts) when a
385 33-frame trained model is tested on 81 frames (second row). 386

387 In contrast, our RoPE alignment design ($[1 - F, 0, 1 - F]$)
388 generalizes to unseen lengths without quality degradations
389 (third row). As demonstrated in Fig 1, our model extrapo-
390 lates to 141 frames (4x training length) and beyond, sup-
391 porting theoretically infinite extrapolation. 392

393 This effectiveness is also quantified in Table 2 (third vs.
394 first column). We observe a 3.4% relative increase in the
395 preservation score. Furthermore, the improved DINO score
396 confirms that our RoPE design better preserves the original
397 video’s spatio-temporal structure during editing. 398

399 **RoPE Design for Motion Alignment.** Setting the tempo-
400 ral index for the reasoning frame latent is a critical design 401

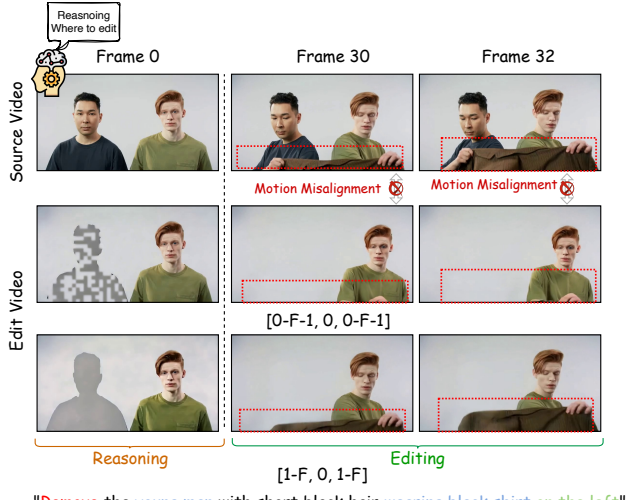


Figure 8. Motion alignment benefit by our rope design.

choice. A naive approach is to set its index to 0, aligning it with the first video frame. This causes two severe issues.

First, it leads to significant motion misalignment (e.g., the subject fails to perform the "lifting clothes" motion in Fig 8, second row). Second, this "0-index" design causes interference with the first editing video frame (also index 0), leading to artifacts where the model incorrectly predicts the first frame as the reasoning frame (Fig 4).

Therefore, we fix the reasoning latent's index to 0, while the source and edited video indices range from 1 to F (denoted as $[1 - F, 0, 1 - F]$). This strategy allows the reasoning frame to provide clear spatial guidance on **where** to edit, without disrupting the video's temporal structure and motion alignment. The improvements across all metrics in Tab 2 (column 3 vs. column 2) validate this design.

Reasoning Frame Format. First, we explore the most suitable color for the reasoning frame mask. As shown in Table 3, we compare three formats: (1) A black mask over the unedit region; (2) A red, 50% transparent highlight, same as veggie [40]; and (3) A pure gray mask (value 127, 0% transparency). The quantitative results show that using a gray mask (column 3) for the edit region yields the best performance.

Furthermore, we argue that the reasoning frame should act as a gradual transition from the source video to the edited video. Therefore, we test progressive gray mask. Instead of a single static mask, we interpolate gray mask reasoning frame and editing frame, with transparency is progressively increased (e.g., 0%, 25%, 50%, 75%). As shown by comparing column 4 and column 3 in Table 3, this progressive gray reasoning frame approach works best.

Qualitatively, as shown in Figure 9, the mask format is critical. The black mask fails the deletion task, while the red mask incorrectly deletes content on the right side. In contrast, our progressive gray mask accurately performs the

Table 3. Ablation on the reasoning frame format.

Color Transparency	Ablation on Reasoning Frame Format			
	Black (bg) (0%)	Red (50%)	Gray (0%)	Gray (0-75%)
<i>GPT-4o Score</i>				
Instruct Follow↑	7.512	7.805	8.069	8.973
Preservation↑	7.034	7.350	7.709	8.203
Quality↑	6.155	6.501	6.926	7.765
Success Ratio↑*	52.170%	60.330%	67.980%	76.36%
<i>Perceptual Quality</i>				
CLIP-T↑	26.550	26.810	27.143	28.000
CLIP-F↑	0.9810	0.9855	0.9890	0.9915
DINO↑	0.9750	0.9790	0.9826	0.9913

intended deletion on the left. We conclude from these experiments that the optimal reasoning format is a gray mask with progressive transparency.

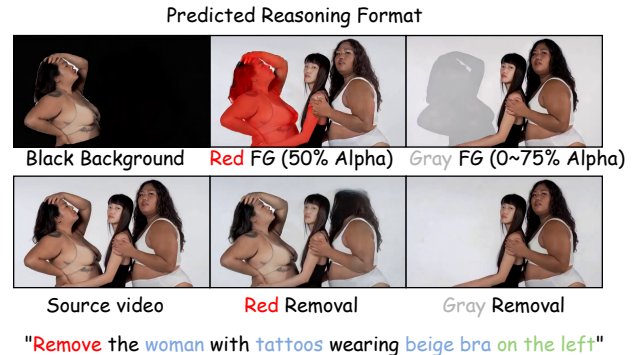


Figure 9. Ablation on reasoning frame format.

5. Conclusion

In this paper, we introduced VideoCoF, a unified model for universal video editing via temporal reasoning. We identified that existing temporal in-context learning approaches often fail due to a lack of explicit spatial cues, leading to weak instruction-to-region mapping and imprecise localization. To address these issues, we proposed the innovative Chain of Frames. CoF compels the video diffusion model to follow a "see, reason, then edit" process by first predicting the editing region before executing the versatile edit. Furthermore, to solve the length generalization challenge, we developed a novel RoPE alignment paradigm that accounts for the reasoning latent. This design enables 4 times exploration in the inference. Experimental results show that VideoCoF achieves SOTA performance using a mere 50k video pairs, validating the efficiency and effectiveness of our temporal reasoning design.

429
430
431

432
433
434
435
436
437
438
439
440
441
442
443
444
445
446
447
448

449 **References**

- 450 [1] Yuxuan Bian, Zhaoyang Zhang, Xuan Ju, Mingdeng Cao,
451 Liangbin Xie, Ying Shan, and Qiang Xu. Videopainter: Any-
452 length video inpainting and editing with plug-and-play con-
453 text control. *arXiv preprint arXiv:2503.05639*, 2025.
- 454 [2] Tim Brooks, Aleksander Holynski, and Alexei A Efros. In-
455 structpix2pix: Learning to follow image editing instructions.
456 In *Proceedings of the IEEE/CVF conference on computer vi-
457 sion and pattern recognition*, pages 18392–18402, 2023.
- 458 [3] Lan Chen, Yuchao Gu, and Qi Mao. Univid: Unifying vi-
459 sion tasks with pre-trained video generation models. *arXiv
460 preprint arXiv:2509.21760*, 2025.
- 461 [4] Jiaxin Cheng, Tianjun Xiao, and Tong He. Consistent video-
462 to-video transfer using synthetic dataset. *arXiv preprint
463 arXiv:2311.00213*, 2023.
- 464 [5] Yuren Cong, Mengmeng Xu, Christian Simon, Shoufa Chen,
465 Jiawei Ren, Yanping Xie, Juan-Manuel Perez-Rua, Bodo
466 Rosenhahn, Tao Xiang, and Sen He. Flatten: Optical flow-
467 guided attention for consistent text-to-video editing. In *Pro-
468 ceedings of the International Conference on Learning Re-
469 presentations (ICLR)*, 2024.
- 470 [6] Yuchao Gu, Yipin Zhou, Bichen Wu, Licheng Yu, Jia-Wei
471 Liu, Rui Zhao, Jay Zhangjie Wu, David Junhao Zhang,
472 Mike Zheng Shou, and Kevin Tang. Videoswap: Customized
473 video subject swapping with interactive semantic point cor-
474 respondence. In *Proceedings of the IEEE/CVF Conference
475 on Computer Vision and Pattern Recognition*, pages 7621–
476 7630, 2024.
- 477 [7] Nicholas Guttenberg. Diffusion with offset noise. [https://www.crosslabs.org/blog/diffusion-with-
478 offset-noise](https://www.crosslabs.org/blog/diffusion-with-offset-noise), 2023.
- 480 [8] Zeyinzi Jiang, Zhen Han, Chaojie Mao, Jingfeng Zhang,
481 Yulin Pan, and Yu Liu. Vace: All-in-one video creation and
482 editing. *arXiv preprint arXiv:2503.07598*, 2025.
- 483 [9] Xuan Ju, Tianyu Wang, Yuqian Zhou, He Zhang, Qing
484 Liu, Nanxuan Zhao, Zhifei Zhang, Yijun Li, Yuanhao Cai,
485 Shaoteng Liu, et al. Editverse: Unifying image and video
486 editing and generation with in-context learning. *arXiv
487 preprint arXiv:2509.20360*, 2025.
- 488 [10] Xuan Ju, Weicai Ye, Quande Liu, Qiulin Wang, Xintao
489 Wang, Pengfei Wan, Di Zhang, Kun Gai, and Qiang Xu.
490 Fulldit: Multi-task video generative foundation model with
491 full attention. *arXiv preprint arXiv:2503.19907*, 2025.
- 492 [11] Takeshi Kojima, Shixiang Shane Gu, Machel Reid, Yutaka
493 Matsuo, and Yusuke Iwasawa. Large language models are
494 zero-shot reasoners. *Advances in neural information pro-
495 cessing systems*, 35:22199–22213, 2022.
- 496 [12] Weijie Kong, Qi Tian, Zijian Zhang, Rox Min, Zuozhuo Dai,
497 Jin Zhou, Jiangfeng Xiong, Xin Li, Bo Wu, Jianwei Zhang,
498 et al. Hunyuanyvideo: A systematic framework for large video
499 generative models. *arXiv preprint arXiv:2412.03603*, 2024.
- 500 [13] Max Ku, Dongfu Jiang, Cong Wei, Xiang Yue, and Wenhui
501 Chen. Viescore: Towards explainable metrics for conditional
502 image synthesis evaluation, 2023.
- 503 [14] Minghan Li, Chenxi Xie, Yichen Wu, Lei Zhang, and
504 Mengyu Wang. Five: A fine-grained video editing bench-
505 mark for evaluating emerging diffusion and rectified flow
506 models. *arXiv preprint arXiv:2503.13684*, 2025.
- 507 [15] Xiaowen Li, Haolan Xue, Peiran Ren, and Liefeng Bo. Dif-
508 fueraser: A diffusion model for video inpainting. *arXiv
509 preprint arXiv:2501.10018*, 2025.
- 510 [16] Xinyao Liao, Xianfang Zeng, Ziye Song, Zhoujie Fu, Gang
511 Yu, and Guosheng Lin. In-context learning with unpaired
512 clips for instruction-based video editing. *arXiv preprint
513 arXiv:2510.14648*, 2025.
- 514 [17] Ilya Loshchilov, Frank Hutter, et al. Fixing weight decay
515 regularization in adam. *arXiv preprint arXiv:1711.05101*, 5
516 (5):5, 2017.
- 517 [18] Chong Mou, Qichao Sun, Yanze Wu, Pengze Zhang,
518 Xinghui Li, Fulong Ye, Songtao Zhao, and Qian He. In-
519 structx: Towards unified visual editing with mllm guidance.
520 *arXiv preprint arXiv:2510.08485*, 2025.
- 521 [19] OpenAI. Hello gpt-4o. Blog post, 2024.
- 522 [20] Pexels. Pexels: Free stock photos, royalty free stock images
523 & videos. <https://www.pexels.com/>, 2025. Ac-
524 cessed: 2025-11-06.
- 525 [21] Chenyang Qi, Xiaodong Cun, Yong Zhang, Chenyang Lei,
526 Xintao Wang, Ying Shan, and Qifeng Chen. Fatezero: Fus-
527 ing attentions for zero-shot text-based video editing. In
528 *Proceedings of the IEEE/CVF International Conference on
529 Computer Vision*, pages 15932–15942, 2023.
- 530 [22] Tianhe Ren, Shilong Liu, Ailing Zeng, Jing Lin, Kun-
531 chang Li, He Cao, Jiayu Chen, Xinyu Huang, Yukang Chen,
532 Feng Yan, Zhaoyang Zeng, Hao Zhang, Feng Li, Jie Yang,
533 Hongyang Li, Qing Jiang, and Lei Zhang. Grounded sam:
534 Assembling open-world models for diverse visual tasks,
535 2024.
- 536 [23] Jianlin Su, Murtadha Ahmed, Yu Lu, Shengfeng Pan, Wen
537 Bo, and Yunfeng Liu. Roformer: Enhanced transformer with
538 rotary position embedding. *Neurocomputing*, 568:127063,
539 2024.
- 540 [24] Wenhao Sun, Rong-Cheng Tu, Jingyi Liao, and Dacheng
541 Tao. Diffusion model-based video editing: A survey. *arXiv
542 preprint arXiv:2407.07111*, 2024.
- 543 [25] DecartAI Team. Lucy edit: Open-weight text-guided video
544 editing, 2025.
- 545 [26] Yuanpeng Tu, Hao Luo, Xi Chen, Sihui Ji, Xiang Bai, and
546 Hengshuang Zhao. Videoanydoor: High-fidelity video ob-
547 ject insertion with precise motion control. In *Proceedings
548 of the Special Interest Group on Computer Graphics and In-
549 teractive Techniques Conference Conference Papers*, pages
550 1–11, 2025.
- 551 [27] Team Wan, Ang Wang, Baole Ai, Bin Wen, Chaojie Mao,
552 Chen-Wei Xie, Di Chen, Feiwu Yu, Haiming Zhao, Jianxiao
553 Yang, et al. Wan: Open and advanced large-scale video
554 generative models. *arXiv preprint arXiv:2503.20314*, 2025.
- 555 [28] Peng Wang, Shuai Bai, Sinan Tan, Shijie Wang, Zhihao Fan,
556 Jinze Bai, Keqin Chen, Xuejing Liu, Jialin Wang, Wenbin
557 Ge, Yang Fan, Kai Dang, Mengfei Du, Xuancheng Ren, Rui
558 Men, Dayiheng Liu, Chang Zhou, Jingren Zhou, and Jun-
559 yang Lin. Qwen2-vl: Enhancing vision-language model's
560 perception of the world at any resolution. *arXiv preprint
561 arXiv:2409.12191*, 2024.

- 562 [29] Cong Wei, Quande Liu, Zixuan Ye, Qiulin Wang, Xintao
563 Wang, Pengfei Wan, Kun Gai, and Wenhua Chen. Univideo:
564 Unified understanding, generation, and editing for videos.
565 *arXiv preprint arXiv:2510.08377*, 2025. 620
566 [30] Jason Wei, Xuezhi Wang, Dale Schuurmans, Maarten
567 Bosma, Fei Xia, Ed Chi, Quoc V Le, Denny Zhou, et al.
568 Chain-of-thought prompting elicits reasoning in large lan-
569 guage models. *Advances in neural information processing
570 systems*, 35:24824–24837, 2022. 621
571 [31] Thaddäus Wiedemer, Yuxuan Li, Paul Vicol, Shixiang Shane
572 Gu, Nick Matarese, Kevin Swersky, Been Kim, Priyank
573 Jaini, and Robert Geirhos. Video models are zero-shot learn-
574 ers and reasoners. *arXiv preprint arXiv:2509.20328*, 2025. 622
575 [32] Haoning Wu, Erli Zhang, Liang Liao, Chaofeng Chen, Jing-
576 wen Hou Hou, Annan Wang, Wenxiu Sun Sun, Qiong Yan,
577 and Weisi Lin. Exploring video quality assessment on user
578 generated contents from aesthetic and technical perspectives.
579 In *International Conference on Computer Vision (ICCV)*,
580 2023. 623
581 [33] Jay Zhangjie Wu, Yixiao Ge, Xintao Wang, Stan Weixian
582 Lei, Yuchao Gu, Yufei Shi, Wynne Hsu, Ying Shan, Xiaohu
583 Qie, and Mike Zheng Shou. Tune-a-video: One-shot tuning
584 of image diffusion models for text-to-video generation. In
585 *Proceedings of the IEEE/CVF international conference on
586 computer vision*, pages 7623–7633, 2023. 624
587 [34] Jay Zhangjie Wu, Xiuyu Li, Difei Gao, Zhen Dong, Jin-
588 bin Bai, Aishani Singh, Xiaoyu Xiang, Youzeng Li, Zuwei
589 Huang, Yuanxi Sun, et al. Cvpr 2023 text guided video edit-
590 ing competition. *arXiv preprint arXiv:2310.16003*, 2023. 625
591 [35] Shitao Xiao, Yueze Wang, Junjie Zhou, Huaying Yuan, Xin-
592 grun Xing, Ruiran Yan, Chaofan Li, Shuteng Wang, Tiejun
593 Huang, and Zheng Liu. Omnigen: Unified image genera-
594 tion. In *Proceedings of the Computer Vision and Pattern
595 Recognition Conference*, pages 13294–13304, 2025. 626
596 [36] Xiangpeng Yang, Linchao Zhu, Hehe Fan, and Yi Yang.
597 Videograins: Modulating space-time attention for multi-
598 grained video editing. In *The Thirteenth International Con-
599 ference on Learning Representations*, 2025. 627
600 [37] Zhuoyi Yang, Jiayan Teng, Wendi Zheng, Ming Ding, Shiyu
601 Huang, Jiazheng Xu, Yuanming Yang, Wenyi Hong, Xiao-
602 han Zhang, Guanyu Feng, et al. Cogvideox: Text-to-video
603 diffusion models with an expert transformer. *arXiv preprint
604 arXiv:2408.06072*, 2024. 628
605 [38] Xixuan Ye, Xuanhua He, Quande Liu, Qiulin Wang, Xintao
606 Wang, Pengfei Wan, Di Zhang, Kun Gai, Qifeng Chen, and
607 Wenhan Luo. Unic: Unified in-context video editing. *arXiv
608 preprint arXiv:2506.04216*, 2025. 629
609 [39] Xixuan Ye, Huijuan Huang, Xintao Wang, Pengfei Wan, Di
610 Zhang, and Wenhan Luo. Stylemaster: Stylize your video
611 with artistic generation and translation. In *Proceedings of
612 the Computer Vision and Pattern Recognition Conference*,
613 pages 2630–2640, 2025. 630
614 [40] Shoubin Yu, Difan Liu, Ziqiao Ma, Yicong Hong, Yang
615 Zhou, Hao Tan, Joyce Chai, and Mohit Bansal. Veg-
616 gie: Instructional editing and reasoning video concepts with
617 grounded generation. In *Proceedings of the IEEE/CVF In-
618 ternational Conference on Computer Vision*, pages 15147–
619 15158, 2025. 631
620 Lvmin Zhang, Anyi Rao, and Maneesh Agrawala. Adding
621 conditional control to text-to-image diffusion models. In
622 *Proceedings of the IEEE/CVF international conference on
623 computer vision*, pages 3836–3847, 2023. 632
624 [42] Zechuan Zhang, Ji Xie, Yu Lu, Zongxin Yang, and Yi Yang.
625 In-context edit: Enabling instructional image editing with in-
626 context generation in large scale diffusion transformer. *arXiv
627 preprint arXiv:2504.20690*, 2025. 633
628 [43] Bojia Zi, Weixuan Peng, Xianbiao Qi, Jianan Wang, Shihao
629 Zhao, Rong Xiao, and Kam-Fai Wong. Minimax-remover:
630 Taming bad noise helps video object removal. *arXiv preprint
631 arXiv:2505.24873*, 2025. 632
632 [44] Bojia Zi, Penghui Ruan, Marco Chen, Xianbiao Qi, Shaozhe
633 Hao, Shihao Zhao, Youze Huang, Bin Liang, Rong Xiao, and
634 Kam-Fai Wong. Se\~norita-2m: A high-quality instruc-
635 tion-based dataset for general video editing by video specialists.
636 *arXiv preprint arXiv:2502.06734*, 2025. 637